

# Modeling of share/soil interaction of a horizontally reversible plow using computational fluid dynamics

Lin Zhu<sup>a,\*</sup>, Jia-Ru Ge<sup>a</sup>, Xi Cheng<sup>a</sup>, Shuang-Shuang Peng<sup>a</sup>, Yin-Yin Qi<sup>a</sup>, Shi-Wu Zhang<sup>b</sup>,  
De-Quan Zhu<sup>a</sup>

<sup>a</sup> Lab of Mechanical Structure & Biomechanics, School of Engineering, Anhui Agricultural University, Hefei 230036, China

<sup>b</sup> Department of Precision Machinery & Precision Instrumentation, University of Science & Technology of China, Hefei 230027, China

Received 27 May 2016; received in revised form 26 October 2016; accepted 17 February 2017

## Abstract

The horizontally reversible plow (HRP) is currently widely used instead of the regular mold-board plow due to its high operational performance. Soil pressure during HRP tillage generally has adverse effects on the plow surface, especially on either the plowshare or the plow-breast. This effect eventually shortens the tool's service life. For this reason, this investigation used a three-dimensional (3D) computational fluid dynamics (CFD) approach to characterize the share/soil interaction and thus assess the effects of different tillage conditions on the interaction. To achieve this goal, a 3D model of the plowshare was first constructed in the commercial software SolidWorks, and soil from Xinjiang, China, was selected and subsequently characterized as a Bingham material based on rheological behaviors. Finally, 3D CFD predictions were performed using the control volume method in the commercial ANSYS code Fluent 14.0 in which the pressure distributions and patterns over the share surface were addressed under different tillage speeds in the range of 2–8 ms<sup>-1</sup> and at operational depths ranging from 0.1 to 0.3 m. The results show that the maximum pressure appeared at the share-point zone of the plowshare and that the increase in soil pressure was accompanied by either higher tool speed or greater operational depth. The calculated results qualitatively agreed with the preliminary experimental evidence at the same settings according to scanning electron microscopy (SEM). Once again, the CFD-based dynamic analysis in this study is demonstrated to offer great potential for the in-depth study of soil-tool interactions by simulating realistic soil matter.

© 2017 ISTVS. Published by Elsevier Ltd. All rights reserved.

**Keywords:** Soil-share interaction; Computational fluid dynamics (CFD); Tillage speed; Operational depth; Horizontally reversible plow (HRP)

## 1. Introduction

In soil excavation processes, tillage tool interaction is the largest energy-consuming operation because it operates via soil cutting with the objective of attaining suitable conditions for crop production (Natsis et al., 2008). The mold-board plow is widely used in tillage, and its plowshare and mold-board are the two main soil-engaging components. Tillage is the mechanical manipulation of the soil in the

tillage layer and results in severe wear on either the plowshare or mold-board (Eltom et al., 2015). The soil pressure distribution and pattern over the plow surface are demonstrated to be strongly associated with the appearance of abrasive wear (Natsis et al., 2008).

The horizontally reversible plow (HRP) is a novel mold-board plow developed by the Xin-Jiang Agricultural Mechanization Institute (XJAMI) of China. The unique advantage of HRP, which is quite different from regular mold-board plows, is that it can facilitate continuous and alternative commuting tillage with excellent operational performance (i.e., steady tilling and orderly soil cutting)

\* Corresponding author.

E-mail address: [zl009@mail.ustc.edu.cn](mailto:zl009@mail.ustc.edu.cn) (L. Zhu).

(Zhu et al., 2006). Fig. 1 shows the commuting tillage process of HRP in real field conditions, where symbols A and B separately denote the two different limited tillage positions of HRP, the pink curves indicate the hypothesized flow of soil clods on the plow surface, and  $n$  is the rotational speed of the basic beam (BB) with respect to the main beam (MB) (Zhu et al., 2006). The rotational speed of the plow body is the same as that of the basic beam (BB) with respect to the main beam (MB) because it is attached to the BB.

In practical HRP tillage operations, severe abrasive wear is always found on the plow surface, especially on either the plowshare or plow-breast. Fig. 2 shows the worn area at the share-point of the plowshare at a tool speed of  $1.67 \text{ ms}^{-1}$  and an operational depth of 0.27 m. This effect not only shortens the tool service life but also affects the plow qualities due to the initial shape changes (Shmulevich, 2010). For the purpose of tool design optimization and performance improvement, a better understanding of the interaction between soil and share is essential to alleviate the worn area that appears on the share-point. In this paper, computational fluid dynamics (CFD) modeling was proposed to investigate the interaction between the soil and the HRP plowshare and examine the wear phenomenon.

Currently, four major methods are available for the investigation of the soil-tool interactions, including empirical and semi-empirical methods, dimensional analysis, the finite element method (FEM) and the distinct element method (DEM) (Karmakar et al., 2007; Barker, 2008). Empirical and semi-empirical models also exist, i.e., mathematical solutions that describe the soil-tool interaction through parametric studies, but they encounter limitations in the pursuit of a better understanding of the soil-tool interaction because they are not based on the real soil failure shapes. The dimensional analysis technique is applied to different parameters of the tillage system, but it is prone to distorted models and obscurity in two-and three-dimensional problems.

The finite element method (FEM) can overcome the drawbacks of the previously mentioned analytical method by supplying the soil-tool interaction with additional

information (such as the progressive soil failure zone and field of stress), but the limitation of FEM is large geometry deformation (Barker, 2008; Karmakar, 2005; Xu et al., 2015). This problem indicates that FEM might not accurately simulate the complex dynamic interactions between the soil and tool. As a potential new technique, the distinct element method (DEM) can implement the particle dynamics interaction to obtain adequate soil reaction forces, but it faces certain difficulties in simulating the real particle size and shape of soils (Shmulevich, 2010). Currently, different authors are working to simulate the soil-tool interaction using DEM, but DEM is limited to simulation of wear distribution on tools (Shmulevich, 2010).

Compared with the above four methods, the main advantage of computational fluid dynamics (CFD) is that it can create a detailed description of the real soil flow distributions (Karmakar, 2005). Hence, CFD is an alternative computational modeling that can assess the pressure distributions that indicate the relative wear of the tool from soil-tool interactions. Considering the soil rheological behavior, Karmakar and Kushwaha (2006) proposed a computational fluid dynamics (CFD) method for soil-tool interaction from a visco-plastic fluid flow perspective and obtained the soil stress patterns around a simple vertical tillage tool and the pressure distributions on the tool surface. However, simulation results of the interaction between the soil and HRP are not available in the literature.

Therefore, this study investigated the feasibility and efficacy of computational fluid dynamic (CFD) modeling in soil-HRP interaction. The CFD-based predictions presented in this paper are primarily focused on the pressure patterns and distributions over the HRP plowshare under high-speed tillage. These numerical simulations were focused on the two key factors, i.e., tool speed and operational depth, that strongly affect the HRP tillage performance (Ranjbar et al., 2013).

## 2. Materials and methods

### 2.1. Model geometry of the plowshare

The plowshare of the HRP has a curved surface, the overall dimensions of which are 0.69 m in length, 0.12 m in width and a 0.01 m maximum height (Zhu et al., 2008). These geometric parameters are strongly correlated with the soil types and the operating conditions, thereby affecting tillage quality and power consumption (Gill and Vanden Berg, 1967). Identification of the plowshare surface is, therefore, essential to better understand the soil-plowshare interaction under real field conditions. In this study, combined feature-based modeling and scanning measurement were used to construct the 3D geometric model of the plowshare. The detailed procedures are depicted as follows. First, the real plowshare surface was scanned using a 3D touch-probe measuring bench (Explorer 07.10.05, Qindao, P.R. China) to determine the Cartesian coordinates of the points in the intersection of

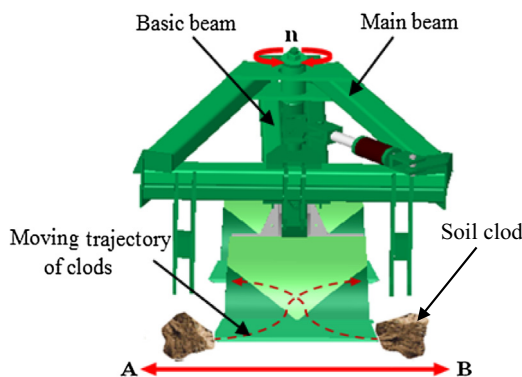


Fig. 1. Commuting tillage process of HRP.

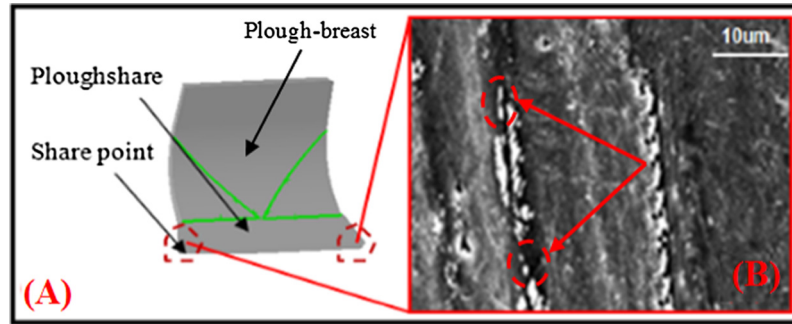


Fig. 2. (A) Plow-surface of HRP, (B) SEM micrograph of the worn plowshare at a tool speed of  $1.67 \text{ ms}^{-1}$  and an operational depth of  $0.27 \text{ m}$ .

the vertical planes with the plow surface (Fig. 3). Second, all points obtained were reproduced and joined by a spline in the 3D design software SolidWorks. Finally, the model geometries of the plowshare surface were created with the feature-based modeling approach (Fig. 4) (Zhu et al., 2016).

## 2.2. Three-dimensional CFD modeling

### 2.2.1. Hypothesis for CFD predictions

Generally, soil rheology in tilling operations is highly complicated, possibly due to variable deformation in the soil-tool interaction. Soil flow is predominantly induced by the stress difference. In other words, the soil flow is initiated as the stress acting on the inter-aggregate contact exceeds the threshold stress, i.e., yield stress. In detail, if the applied stress is less than the yield stress, the soil flow acts as a viscous-plastic fluid, and if the stress exceeds the yield stress, the soil flows in a manner similar to a fluid (Terzaghi, 1948; Bird et al., 1983). In the foregoing process, the relationship between stress and soil flow rate is non-linear, and the soil flow pattern can be considered as a laminar flow in accordance with the high molecular weight

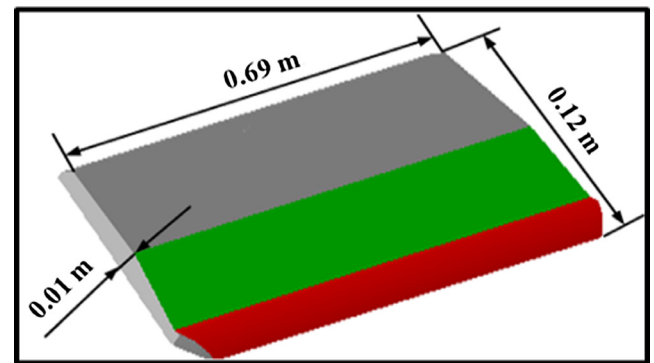


Fig. 4. Three-dimensional model of the plowshare.

(Terzaghi, 1948; Desai and Phan, 1980; White, 1999). For this reason, the dynamic process of tillage can be studied via non-Newtonian flow behavior from a fluid flow perspective. This approach indicates that the soil-tool interaction can be viewed as an external flow over a bluff body (Karmakar, 2005). To investigate the flow interaction, a volume of fluid is commonly defined for the mechanical characteristics of the specific volume fraction. Additionally, because the volume fraction consists of soil, water and air, a multiphase fluid flow method should be considered (Barker, 2008; Terzaghi, 1948).

### 2.2.2. CFD-based flow model

During the soil/HRP interaction, the plowshare is considered as a stationary tool located within a visco-plastic flowing domain. This domain represents the soil, i.e., the



Fig. 3. Three-dimensional touch-probe measuring.

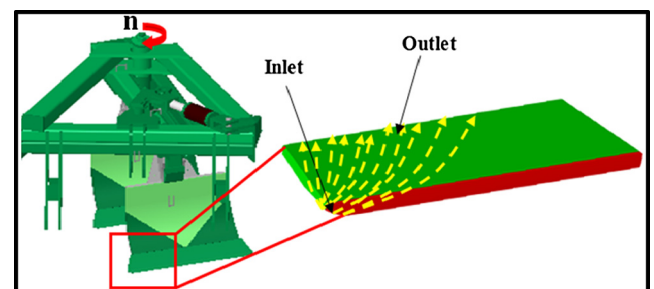


Fig. 5. Soil flow pattern on the plowshare surface (Zhu et al., 2016).

plowshare is placed in a free surface domain and acts as a bluff body obstruction. Fig. 5 schematically illustrates the soil flow pattern when the plow-body is operated from right to left. Note that this flow configuration is based on the real tillage tool interaction. As shown in Fig. 5, the primary domain of the soil flow is a surface with an area of 0.0379 m<sup>2</sup> (see the yellow<sup>1</sup> zone in Fig. 5).

### 2.2.3. Governing equations and constitutive relations

The CFD-based numerical simulation approach is used to investigate particle movements in a system, including velocity and stress distribution fields in a well-defined form to which the mass and momentum conservation equations are applied, respectively (Desai and Phan, 1980; White, 1999). Due to the effectiveness of the Navier-Stokes equations for any fluid flow, the soil-tool flow interaction can also be investigated by incorporating non-Newtonian parameters into these basic equations (Barker, 2008; Xu et al., 2015).

We apply the mass conservation through the control volume, and thus the continuity equation is written as follows:

$$\frac{\partial \rho}{\partial t} + \frac{\partial}{\partial x_i}(\rho \mu_i) = 0 \quad (1)$$

where  $t$ ,  $\rho$ ,  $\mu_i$  and  $x_i$  are the flow time, fluid density, directional velocity and displacement of the fluid, respectively.

The variation in the time rate of the density at any flow location is balanced by the net mass flux at the corresponding point. For simplification, if the soil is considered incompressible and assumed as a single-phase continuous medium with a constant density,  $\rho$  should be a bulk density with any pore water in the soil. Thus, Eq. (1) can be reduced to the following form (see Eq. (2)), which indicates that the volume of the differential fluid element does not change.

$$\frac{\partial}{\partial x_i}(\rho \mu_i) = 0 \quad (2)$$

According to Newton's second law, the relationship between the acceleration of a fluid element and the net force acting on it can be presented (Desai and Phan, 1980; White, 1999):

$$\rho \frac{D\mu_i}{Dt} = \rho g - \frac{\partial P}{\partial x_i} + \frac{\partial \tau_{ij}}{\partial x_j} \quad (3)$$

where  $D/Dt$  is the function of substantial or total derivative,  $g$  is the acceleration of gravity,  $P$  is the hydrostatic pressure, and  $\tau_{ij}$  is the shear stress tensor.

The material or substantial derivative is a function of both temporal and spatial changes and can be written as follows (White, 1999):

$$\frac{D\mu_i}{Dt} = \frac{\partial \mu_i}{\partial t} + \mu_j \frac{\partial \mu_i}{\partial x_j} \quad (4)$$

Eq. (3) indicates that the acceleration of the fluid element is balanced jointly by the gravitational force, pressure (hydrostatic stress) and viscous (hydrodynamic) stress. Therefore, it is concluded that the different aspects of the real soil-tool dynamics interaction (such as draft force, pressure and soil failure due to visco-plastic deformation) can be characterized using the fluid flow method.

For a Bingham plastic fluid, the generalized stress-strain rate can be written as follows (Desai and Phan, 1980; White, 1999):

$$\tau_{ii} = \sigma_i = 2\mu \frac{\partial \mu}{\partial x} \quad (5)$$

$$\tau_{ij} = \tau_y + \mu \left( \frac{\partial u_i}{\partial x_j} + \frac{\partial \mu_j}{\partial x_i} \right) = \tau_y + \mu \gamma \quad \text{for } |\tau_{ij}| > \tau_y \quad (6)$$

$$\gamma = 0 \quad \text{for } |\tau_{ij}| \leq \tau_y \quad (7)$$

where  $\gamma$  is the shear rate,  $\tau_i$  is the yield stress, and  $\mu$  is the constant viscosity or plastic viscosity.

Note that in this study, the soil yield stress was assumed independent of position or orientation of the fluid particles to satisfy the homogeneity and isotropy of the visco-plastic fluid.

### 2.2.4. Numerical modeling and boundary conditions

For the purpose of examining the soil flow around the plowshare, different tillage speeds, operational depths and isothermal conditions were all included in this study. The control volume method in a commercially available CFD code, i.e., ANSYS Fluent 14.0 (ANSYS FLUENT), was used to predict the pressure distributions and patterns over the share-surface of the HRP. Fig. 6 illustrates the CFD grid of the plowshare with 5399 tetrahedral cells in Gambit 2.4 (ANSYS FLUENT).

During HRP tillage, the soil is first drawn into the computational domain through the share-point with an inlet velocity and mostly flows out from the center section of the plowshare (Figs. 5 and 6). Thus, the detailed boundary conditions for the CFD simulations are specified as follows: (1) The velocity component normal to the inlet boundary is 2–8 m/s, (2) the pressure boundary is applied at the outlet, (3) no slip occurs at the wall boundaries at

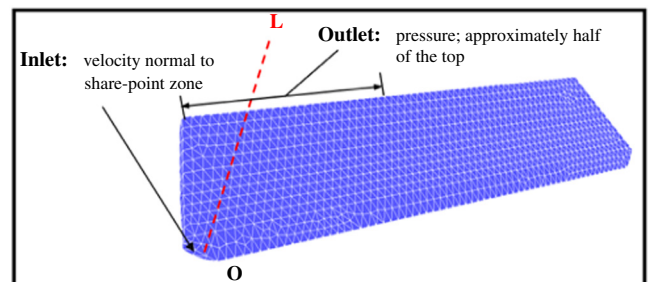


Fig. 6. CFD grid of the plowshare.

<sup>1</sup> For interpretation of color in Figs. 2, 5, 7, and 11, the reader is referred to the web version of this article.



the bottom or sides of the plowshare, and (4) the free-surface grid movement is confined in the 3D surface region. In addition, the different operational depths of HRP, i.e.,  $H = 0.1$ – $0.3$  m, were also considered in the computational domain. For all calculations, the numerical results were based on the criterion that the residual of each equation should be smaller than  $1.0 \times 10^{-5}$ .

### 2.2.5. Soil parameters for CFD prediction

For real soil with water and air, as depicted previously, the multiphase fluid flow should be considered. However, for simplicity, a single-phase laminar flow was used to characterize the dynamic interaction between the soil and plowshare in this study. Currently, the HRP is widely used in Xin-Jiang in China. According to the corresponding soil properties (a bulk density of  $1453 \text{ kg m}^{-3}$ , a cone index value of  $398 \text{ kPa}$  and a moisture content of  $17\%$ ), the soil presented in this work was characterized as an incompressible, isotropic and homogeneous Bingham material (Gill and Vanden Berg, 1967). Thus, the dynamic parameters of the soil can be determined using the strain-rate based soil torsional rheometer developed by XJAMI (Zhu et al., 2008). The measured dynamic parameters of the soil for CFD modeling were a yield stress of  $15.5 \text{ kPa}$  and an apparent viscosity of  $167 \text{ kPa s}$ . Note that during the tests, two independent variables that influence the yield stress and viscosity, i.e., soil moisture content and cone index, respectively, were considered.

## 3. Results and discussion

According to Ranjbar et al. (2013), Terzaghi (1948), the soil pressure distribution and pattern during tillage have significant effects on the wear phenomena of the plowshare surface and hence on the tool life. Both tool speed and operational depth are two important tillage conditions. The following CFD-based predictions, therefore, focused on pressure patterns and distributions over the plowshare under the different tool speeds and operational depths.

Fig. 7 shows the CFD-based prediction under different operational depths, i.e.,  $0.1$ ,  $0.2$ , and  $0.3$  m and different tool speeds, i.e.,  $2$ ,  $4$ ,  $6$ , and  $8 \text{ ms}^{-1}$ . The red, green and blue colors in Fig. 7 respectively represent the maximum, median and minimum pressure sections over the plowshare surface. The results showed that for the pressure distribution and pattern over the plowshare, reasonably good

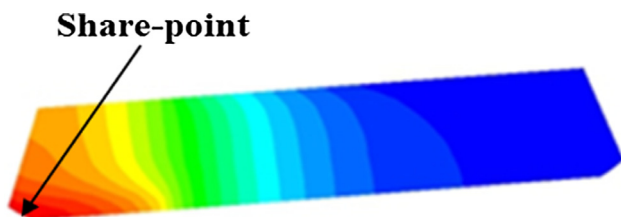


Fig. 7. CFD-based prediction of the plowshare at different operational depths and various tool speeds.

Table 1

Maximum pressures over the plowshare at different operational depths ( $H$ ) and different tool speeds ( $V$ ).

$P_{\max}$	$H = 0.1 \text{ m}$	$H = 0.2 \text{ m}$	$H = 0.3 \text{ m}$
$V = 2 \text{ ms}^{-1}$	17.6 MPa	21.6 MPa	30.5 MPa
$V = 4 \text{ ms}^{-1}$	35.3 MPa	43.4 MPa	61.4 MPa
$V = 6 \text{ ms}^{-1}$	53.2 MPa	65.3 MPa	92.7 MPa
$V = 8 \text{ ms}^{-1}$	71.3 MPa	87.4 MPa	124 MPa

qualitative agreement was observed between the two tillage conditions, i.e., tool speed and operational depth. In other words, the maximum pressures both appeared at the share-point of the plowshare. However, a discrepancy in magnitude was noted for the maximum pressure. The detailed values are listed in Table 1.

Fig. 8 plots the pressure variations over the plowshare with changes in distance at the different operational depths ( $H$ ), i.e.,  $0.1$ ,  $0.2$  and  $0.3$  m. The distance ( $D$ ) presented in this work is the length between any point, e.g., point A on the normal L of the share-point section and the share-point O, as shown in Figs. 6 and 9.

As observed, for the range of tool speeds from  $2$  to  $8 \text{ ms}^{-1}$ , a greater operational depth was accompanied by higher pressure at the plowshare, and the maximum pressures all appeared at the share-point section, especially close to the share-point. At operational depths ranging from  $0.1$  m to  $0.3$  m, the maximum pressure approximately increased from  $17$ ,  $34$ ,  $52$ ,  $70 \text{ MPa}$  to  $30$ ,  $60$ ,  $90$ , and  $120 \text{ MPa}$ , respectively, corresponding to tool speeds of  $2$ ,  $4$ ,  $6$ , and  $8 \text{ ms}^{-1}$ . Furthermore, for any tool speed and operational depth, as shown in Fig. 8, the highest pressure at the share-point gradually decreased with the distance from the share-point.

Fig. 10 shows the pressure variations on the plowshare with distance under different tillage speeds, i.e.,  $2$ ,  $4$ ,  $6$  and  $8 \text{ ms}^{-1}$ . Note that the distance presented has the same meaning as in Fig. 8. As observed, at operational depths ranging from  $0.1$  m to  $0.3$  m, greater tool speed also resulted in higher pressure on the plowshare. The maximum pressures on the plowshare all appeared at the share-point. For tool speeds in the range of  $2$ – $8 \text{ ms}^{-1}$ , the highest pressures approximately increased from  $17$ ,  $21$ , and  $30 \text{ MPa}$  to  $70$ ,  $85$ , and  $120 \text{ MPa}$ , respectively, corresponding to operational depths of  $0.1$ ,  $0.2$  and  $0.3$  m. In addition, similar to in the information shown in Fig. 8, for any tool speed and operational depth, the variation tendency of the pressures on the plowshare was that the highest pressure at the share-point also gradually decreased with the distance from the share-point.

It can be concluded from Figs. 7, 8 and 10 that for different tillage speeds and operational depths, the pressure on the plowshare increases with either tillage speed or operational depth and that the maximum pressures on the plowshare all appear at the share-point zone. This observation might be attributed to the fact that the share-point is the main soil engagement section of the plowshare, where

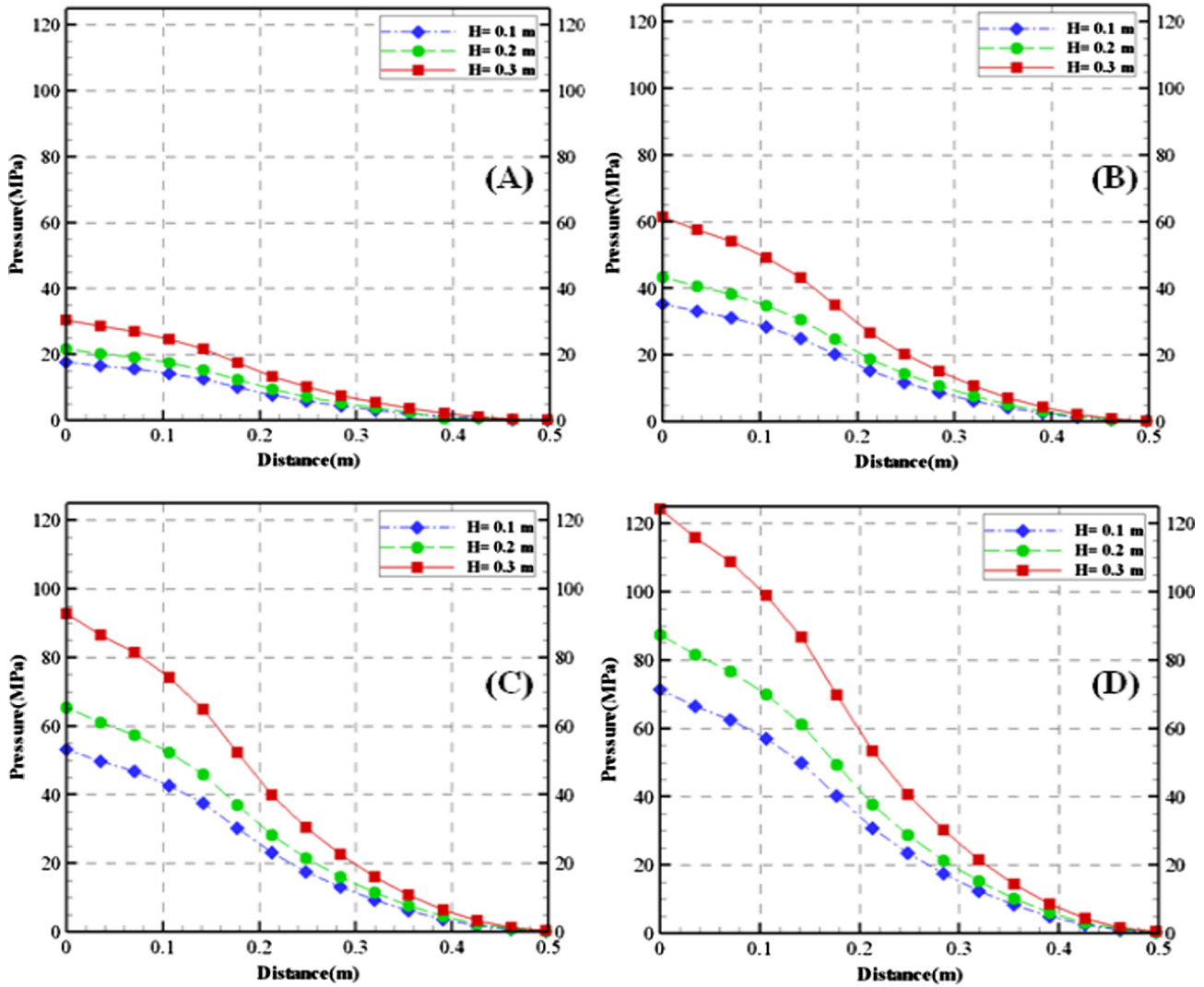


Fig. 8. Pressure variation on the share-point with change in distance at different operational depths ( $H$ ) and a constant tillage speed of (A)  $2 \text{ ms}^{-1}$ , (B)  $4 \text{ ms}^{-1}$ , (C)  $6 \text{ ms}^{-1}$  and (D)  $8 \text{ ms}^{-1}$ .

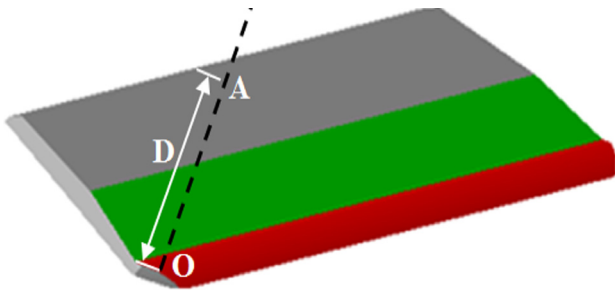


Fig. 9. Distance between any point on the normal of the share-point section and the share-point of the plowshare.

a large amount of energy is necessary to cut, break down and reduce the clod size. This action eventually leads to the greatest stress concentration in the soil surrounding the share-point zone.

Generally, the soil front propagation or soil disturbance zone in the tilling operation can be interpreted via the

pressure distribution on the tool surface (Terzaghi, 1948; Anonymous, 2001; Adichi and Yoshioka, 1973). Thus, the soil plastic flow section can be considered as the soil disturbance zone with particular soil stresses. Consequently, the maximum soil stress in the flow domain indicates the highest pressure on the tool surface. The share-point is the main soil engagement zone of the plowshare. According to Coulomb's passive earth pressure theory, a succession of the shear planes leads to block separation of the soil mass, which in turn causes shear failure to initiate from the tool cutting edge (Anonymous, 2001). It is, therefore, inferred that the maximum load on the plowshare due to soil-tool interaction lies at the share-point zone, as numerically demonstrated by CFD modeling in Figs. 7, 8 and 10, and thus supports the assumptions of Coulomb's passive earth pressure theory.

From a fluid flow perspective, because the soil in this study was modeled using the Bingham constitutive law, a characteristic peculiarity concerning the fluidity of the

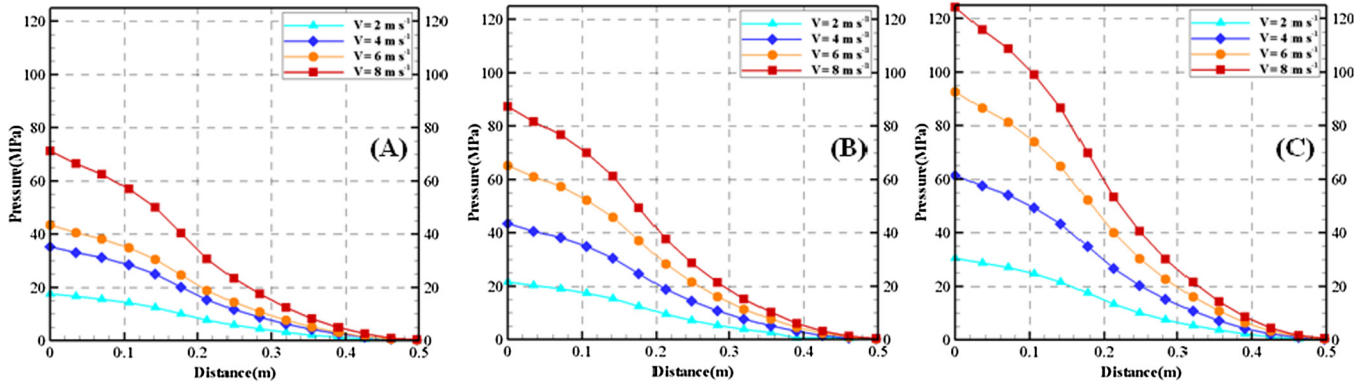


Fig. 10. Pressure variation on the plowshare with change in distance at the different tillage speeds ( $V$ ) and a constant operation depth of (A) 0.1 m, (B) 0.2 m and (C) 0.3 m.

visco-plastic medium appears at the boundaries between the tool and soil. According to Adichi and Yoshioka (1973), these boundaries can divide the flow fields into fluid regions and rigid regions. The fluid or plastic flow regions are located close to the boundary of the flow, where the pressure gradient is rather high. Hence, the maximum pressure at the share-point zone of the plowshare might be caused by the stagnation point of fluid flow.

#### 4. Comparison of numerical and preliminary measurements

The CFD-based simulations in this study showed that all of the maximum pressures appeared at the share-point zone of the plowshare. The preliminary measurements from SEM showed that at a tool speed of  $1.67 \text{ ms}^{-1}$  and operational depth of 0.27 m, the most severe wear area on the plowshare also occurred at the share-point section (Fig. 2). This location is where the maximum pressure on the plowshare lies, as shown in Figs. 7, 8 and 10. At the same time, the CFD-based predictions in this study further showed that the maximum pressure at the share-point zone was increased with either tillage speed or operational depth. Under similar tillage conditions, for example, when the operational depth was increased from 0.2 m to 0.3 m at a constant tool speed of  $2 \text{ ms}^{-1}$ , the maximum pressure at

the share-point was increased from 21.6 MPa to 30.5 MPa (Table 1, Fig. 11(A) and (B)). The recent experimental measurements also validated that at a tool speed of  $1.67 \text{ ms}^{-1}$ , a more severely worn area (compared to Fig. 2) appeared at the share-point when the operational depth was increased from 0.27 m to 0.36 m (see the red arrows in Figs. 2 and 11(C)). The highest pressure incurs the most severe wear on the tool surface in the soil-cutting process (Koolen, 1983). Based on qualitative comparisons among Figs. 2 and Figs. 7 and 11, we infer that the most severe wear over the plowshare surface under other tool speeds and operational depths should also appear at the share-point section and might even be more severe than that shown in Fig. 2.

In general, the overall trend of the numerical results shows good qualitative agreement with the measurements. This outcome once again demonstrates that CFD modeling can be feasibly and effectively used to study soil-tool interaction and hence tool design improvement. However, the current results suggest further investigations. First, the adequate values of the more severe wear areas on the plowshare under the different tool speeds and operational depths were numerically determined using the maximum pressure profiles obtained in this study. Second, additional experimental work is also required to investigate the wear

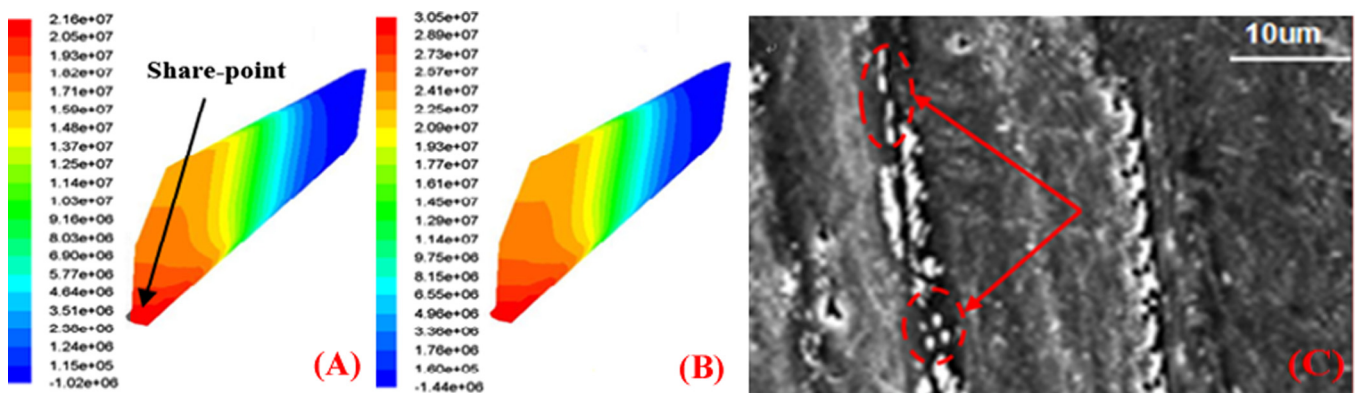


Fig. 11. Comparison between CFD predictions and the experiment at similar tillage conditions.

phenomenon on the plowshare, including pressure distribution measurements and SEM-based analyses under the identified operation conditions. Higher pressure indicates a stronger soil-tool interaction and thus leads to more severe wear and shorter tool service life.

## 5. Conclusions

Based on the merits and weaknesses of the existing soil-tool modeling methods, 3D CFD predictions were proposed to investigate the flow interaction between the soil and plowshare during HRP high-speed tillage. This study focused on the pressure patterns and distributions over the plowshare under different tillage speeds, i.e.,  $2\text{--}8\text{ ms}^{-1}$ , and operational depths, i.e.,  $0.1\text{--}0.3\text{ m}$ . The numerical simulations demonstrated that the maximum pressures all appeared at the share-point zone of the plowshare and that the pressures at the share-point increased with either tillage speed or operational depth. Preliminary and further measurements both showed that the most severe wear areas appeared at the share-point section of the plowshare and that the wear areas at the share-point became more severe with increasing operational depth. Because the highest pressure is strongly associated with the most severe wear phenomenon for the plowshare, the CFD-based predictions in this study show good qualitative agreement with the preliminarily measured evidence from SEM. CFD-based modeling in the tillage area is once again demonstrated to be feasible and effective for the in-depth study of soil-tool interactions by simulating realistic soil manners. The research results in this study offer a new dimension for agricultural tool design and especially for HRP design.

## Acknowledgments

The authors acknowledge financial support for this work from the National Natural Science Foundation of China (Grant No. 51575003), the Anhui Provincial Natural Science Foundation (Grant No. 1508085ME71) and the Key Project of Anhui Education Committee (Grant No. KJ2015A031). The authors also thank the reviewers for their valuable input.

## References

Adichi, K., Yoshioka, N., 1973. On creeping flow of a visco-plastic fluid past a circular cylinder. *Chem. Eng. Sci.* 28 (1), 215–226.  
Anonymous, 2001. Earth pressure theory and applications. In: *Trenching and Shoring Manual*. California Department of Transportation, Sacramento, CA, USA.

Barker, M.E., 2008. Predicting Loads on Ground Engaging Tillage Tools Using Computational Fluid Dynamics. PhD Thesis. Iowa State University, Iowa, USA.  
Bird, R.B., Dai, G.C., Yarusso, B.J., 1983. The rheology and flow of visco-plastic materials. *Rev. Chem. Eng.* 529 (1), 1–70.  
Desai, C.S., Phan, H.V., 1980. Computational methods in non-linear mechanics. North Holland Publishing Company, 205–245.  
Eltom, A.E. Farid, Ding, Weimin, Ding, Qishuo, Ali, Abu baker B., Adam, B. Eisa, 2015. Effects of trash board on moldboard plow performance at low speed and under two straw conditions. *J. Terramech.* 59, 27–34.  
Gill, W.R., Vanden Berg, G.E., 1967. Soil dynamics in tillage and traction. In: *Agriculture Handbook No. 316*. Agricultural Research Service, U. S. Department of Agriculture, 511.  
Karmakar, S., 2005. Numerical Modeling of Soil Flow and Pressure Distribution on a Simple Tillage Tool Using Computational Fluid Dynamics. PhD Thesis. University of Saskatchewan, Canada.  
Karmakar, S., Kushwaha, R.L., 2006. Dynamic modeling of soil-tool interaction: an overview from a fluid flow perspective. *J. Terramech.* 43, 411–425.  
Karmakar, S., Kushwaha, R.L., Laguë, C., 2007. Numerical modeling of soil stress and pressure distribution on a flat tillage tool using computational fluid dynamics. *Biosyst. Eng.* 97, 407–414.  
Koolen, A.J., 1983. *Agricultural Soil Mechanics*. Advanced Series in Agricultural Sciences. Springer-Verlag, Berlin.  
Natsis, A., Petropoulos, G., Pandazaras, C., 2008. Influence of local soil conditions on moldboard plowshare abrasive wear. *Tribol. Int.* 41, 151–157.  
Ranjbar, I., Rashidi, M., Najjarzadeh, I., Niazkhani, A., Niyazadeh, M., 2013. Modeling of moldboard plow draft force based on tillage depth and operation speed. *Middle-East J. Sci. Res.* 17, 891–897.  
Shmulevich, I., 2010. State of the art modeling of soil-tillage interaction using discrete element method. *Soil Tillage Res.* 111, 41–53.  
Terzaghi, K., 1948. *Theoretical Soil Mechanics*. Chapman and Hall, London.  
White, F.M., 1999. *Fluid Mechanics*, 4th ed. WCB/McGraw-Hill, Columbus, OH, USA.  
Xu, Lichao, Zhang, Shiwu, Jiang, Nan, Xu, Ronald X., 2015. A hybrid force model to estimate the dynamics of curved legs in granular material. *J. Terramech.* 59, 59–70.  
Zhu, Lin, Yin, Chen-Long, Chen, Fa, 2006. The application of virtual prototype technology on analyzing the kinetic and dynamic characteristic of horizontally reversible plow. *Int. J. Jpn. Soc. Mech. Eng. Ser. C* 41, 247–252.  
Zhu, Lin, Xu, Jin-Liang, Yin, Cheng-Long, Kong, Fan-Rang, Kong, Xiao-Ling, 2008. Design of plowshare of horizontal reversible plow with computer simulation technique. *J. Syst. Simul.* 20 (13), 3455–3458.  
Zhu, Lin, Peng, Shuang-Shuang, Xi-Cheng, Qi, Yin-Yin, Zhang, Wen-Feng, Xu, Liang-Yuan, 2016. Virtual assembly geometric semantics and constraint for an improved three-dimensional model of horizontally reversible plow. *Int. J. Mech. Sci. Technol.* 30 (1), 257–266.  
Zhu, Lin, Peng, Shuang-Shuang, Cheng, Xi, Qi, Yin-Yin, Ge, Jia-Ru, Yin, Cheng-Long, Jen, Tien-Chien, 2016. Combined finite element and multi-body dynamics analysis of effects of hydraulic cylinder movement on plowshare of Horizontally Reversible Plow. *Soil Tillage Res.* 163, 168–175.